Valley dynamics probed through charged and neutral exciton emission in monolayer WSe_2

G. Wang, L. Bouet, D. Lagarde, M. Vidal, A. Balocchi, T. Amand, X. Marie, and B. Urbaszek
Université de Toulouse, INSA-CNRS-UPS, LPCNO, 135 Avenue de Rangueil, 31077 Toulouse, France
(Received 3 June 2014; revised manuscript received 28 July 2014; published 18 August 2014)

Optical interband transitions in monolayer transition metal dichalcogenides such as WSe_2 and MoS_2 are governed by chiral selection rules. This allows efficient optical initialization of an electron in a specific K valley in momentum space. Here we probe the valley dynamics in monolayer WSe_2 by monitoring the emission and polarization dynamics of the well-separated neutral excitons (bound electron-hole pairs) and charged excitons (trions) in photoluminescence. The neutral exciton photoluminescence intensity decay time is about 4 ps, whereas the trion emission occurs over several tens of ps. The trion polarization dynamics shows a partial, fast initial decay within tens of ps before reaching a stable polarization of ≈20%, for which a typical valley polarization decay time of the order of 1 ns can be inferred.

DOI: 10.1103/PhysRevB.90.075413 PACS number(s): 78.60.Lc, 78.66.Li

I. INTRODUCTION

In strong analogy to graphene, the physical properties of transition metal dichalcogenides (TMDCs) change drastically when thinning the bulk material down to one monolayer (ML) [1]. The closely related ML materials WSe_2, MoS_2, $MoSe_2$, and WS_2 [2] have a direct band gap in the visible region [3–5] and show strong optical absorption. ML WSe_2 is an exciting, atomically flat, two-dimensional material for electronics [6,7], nonlinear optics [8], and optoelectronics [9,10], just as ML MoS_2 [10–12]. Current micro-and nanoelectronics are based on the manipulation of the electron charge and spin. ML TMDCs provide unique and convenient access to additionally controlling the electron valley degree of freedom in k space in the emerging field of "valleytronics" [13–15].

The circular polarization (σ^+ or σ^-) of the absorbed or emitted photon can be directly associated with selective carrier excitation in one of the two nonequivalent K valleys (K_+ or K_-, respectively) [2,13,16,17] see Fig. 2(a). The valley polarization is protected by the strong spin-orbit splitting in the valence and conduction band [13,18–20], leading in principle to a high stability for the valley degree of freedom. The high circular photoluminescence (PL) polarization degree reported in time-integrated measurements in ML MoS_2 [16,21–25] and ML WSe_2 [21] seems to confirm this prediction.

The stability of the created valley polarization is crucial for manipulating the electron valley degree of freedom in transport measurements or with successive laser pulses in optical control schemes, where excitonic effects are important [26,27]. Recent time-resolved studies show PL emission times in the picosecond range [28,29] and pump-probe measurements in ML MoS_2 have shown polarization decay times in the ps range [30,31], corresponding to fast relaxation of the valley index. In these experiments on ML MoS_2 the neutral exciton (X^0) and the charged exciton (trion) emission cannot be clearly spectrally separated due to the broad transitions, although the evolution of the valley polarization is expected to be distinctly different for the two complexes. The neutral excitons in different K valleys are coupled by a Coulomb exchange [32], which can lead to intervalley scattering [33–35]. The trion polarization is expected to be far more stable as intervalley scattering demands, in this case, spin flips of individual carriers, which are energetically and spin forbidden. This would make the trion an excellent candidate for optically initialized valley Hall experiments [34]. However, the trion valley dynamics in ML TMDCs is so far unexplored.

In time-resolved PL (TRPL) experiments we uncover marked differences between the X^0 and the trion valley dynamics in ML WSe_2 as the spectrally well-separated transition can be analyzed independently at low temperature [see Fig. 2(e)]. We measure a trion emission time of ≈18 ps [36]. Following optical initialization with a circularly polarized laser, the trion PL emission reaches a stable polarization within about 12 ps. For the strong remaining polarization we can infer a decay time of the order of 1 ns. This is a direct experimental signature of the temporal stability of optically generated valley polarization. In contrast, the neutral exciton emission and polarization decay within a few ps. We also clearly identify localized excitons via their characteristically long emission times due to the lower dipole oscillator strength.

II. SAMPLES AND EXPERIMENTAL SETUP

Monolayer WSe_2 flakes are obtained by micromechanical cleavage of a bulk WSe_2 crystal [37] (from 2D Semiconductors, USA) on 90 nm SiO_2 on a Si substrate [see Fig. 1(a)]. The 1 ML region is identified by optical contrast and very clearly in PL spectroscopy. Experiments between $T = 4$ and 300 K are carried out in a confocal microscope optimized for polarized PL experiments [38]. The WSe_2 flake is excited by picosecond pulses generated by a tunable frequency-doubled optical parametric oscillator (OPO) synchronously pumped by a mode-locked Ti:Sa laser. The typical pulse and spectral width are 1.6 ps and 3 meV, respectively; the repetition rate is 80 MHz. The laser power has been kept in the μW range in the linear absorption regime [see Fig. 2(b)]. The laser wavelength can be tuned between 500 and 740 nm. The detection spot diameter is ≈1 μm. For time-integrated experiments, the PL emission is dispersed in a spectrometer and detected with a Si-CCD camera. For time-resolved experiments, the PL signal is dispersed by an imaging spectrometer and detected by a synchroscan Hamamatsu streak camera with an overall time resolution of 4 ps. The PL intensity components circularly co- and counterpolarized with respect to the excitation laser polarization σ^+ are recorded. This allows direct access to the exciton populations in the K_+ and K_- valley, respectively.

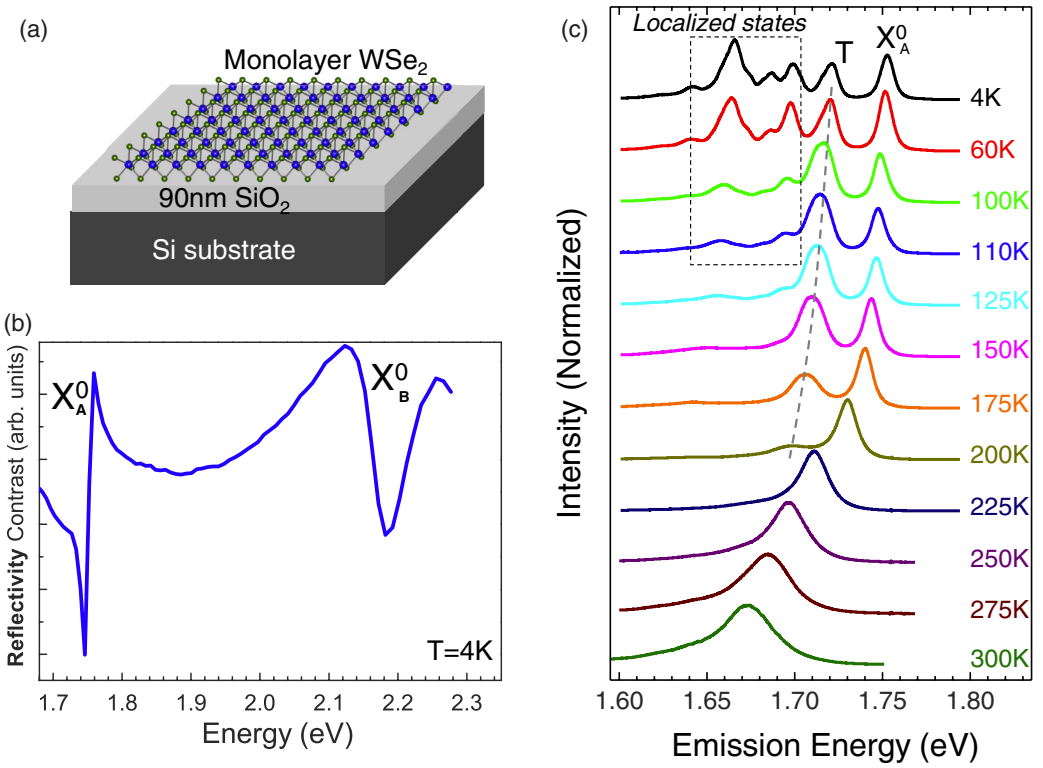

FIG. 1. (Color online) (a) Investigated sample structure, (b) reflectivity measurements at $T = 4$ K, and (c) PL emission of the neutral exciton X^0, the trion (T), and localized states as a function of temperature.

Hence the PL polarization P_c is defined as $P_c = \frac{I_{\sigma+}-I_{\sigma-}}{I_{\sigma+}+I_{\sigma-}}$, analyzed by a quarter-wave plate placed in front of a linear polarizer. Here $I_{\sigma+}(I_{\sigma-})$ denotes the intensity of the right (σ^+) and left (σ^-) circularly polarized emission.

III. EXPERIMENTAL RESULTS

For PL experiments the laser excitation energy is $E_{\text{Laser}} = 1.893$ eV, which is 140 meV above the neutral A-exciton emission energy and clearly below the B-exciton absorption, as confirmed in reflectivity measurements in Fig. 1(b). The time-integrated PL emission at $T = 4$ K of the WSe_2 monolayer stems from the recombination of X^0, trions, and localized excitons. The emission attributed to localized states is no longer detectable for temperatures above 125 K in Fig. 1(c), confirming the intrinsic nature of only the X^0 and trion (T) transitions. Note that the temperature dependent PL was performed at a sample position slightly different from the measurements in Figs. 2–4, which only changes the relative intensity of the localized states. The PL recorded in Fig. 2 is very similar to the emission reported for this system in Ref. [21], where a bias was applied to the ML WSe_2. Considering the commonly observed residual n-type doping, the trion charge is most likely to be negative, as assumed for the discussion below [39].

The identification of the transitions is based on the polarization analysis shown in Figs. 2(c) and 2(d). Under linearly polarized laser excitation, only the highest energy peak shows linear polarization in emission and is therefore ascribed to the X^0, as a coherent superposition of valley states is created [21]. This observation of exciton alignment is independent of the direction of the incident laser polarization, which confirms that the observed linear polarization is not due to macroscopic birefringence in the sample. The strong remaining coherence in Fig. 2(d) following nonresonant excitation is linked to the direct optical generation of the neutral exciton X^0 $2s$ state for the laser energy used [40], energetically below the free carrier absorption and well below the B exciton. Under circularly polarized excitation in Fig. 2(c), the two highest energy transitions are strongly polarized, as expected for the $X^0$and the trion. The clear separation by 30 meV of the trion [PL full width at half maximum (FWHM) 15 meV] and neutral exciton (PL FWHM 10 meV) is a major advantage compared to current MoS_2 ML samples for the independent investigation of the valley dynamics, also possible in ML $MoSe_2$ [41]. Energetically below the trion emission we record two emission peaks that we assign to localized exciton complexes that disappear when raising the temperature and that are accordingly labeled $L1$ and $L2$.

In TRPL experiments we observe striking differences between the main transitions, as can be seen in Figs. 2(e) and 3. We first discuss the emission times that can be compared in Fig. 3. The main X^0 emission time cannot be resolved by our experiment; it decays within 4 ps, as shown in Fig. 3, in a very similar way to ML MoS_2 [28]. As a result of the short PL emission time, the coherence time could be as short as a few ps and still result in a strong linear polarization degree of the time-integrated PL [21]. Whether the short X^0 emission time is limited by radiative recombination (in this system with predicted [26,27] and measured [40] exciton binding energies of several hundred meV) or by nonradiative processes is still an open question. The two to three orders of magnitude weaker

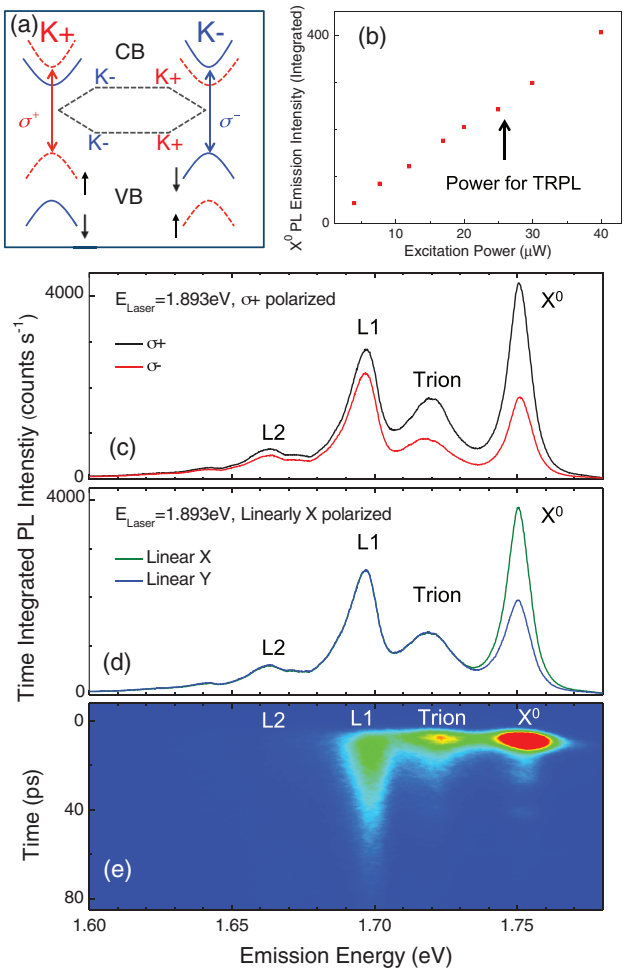

FIG. 2. (Color online) (a) Optical interband selection rules for monolayer WSe_2 according to Ref. [18]. (b) Investigated sample structure. (c) Laser polarization σ^+ and $E_{\text{Laser}} = 1.893$ eV. PL emission of ML WSe_2 at $T = 4$ K, and the X^0, trion, and localized states are marked. Black (red): $\sigma^+(\sigma-)$ polarized. (d) Linear laser polarization X. Green (blue) corresponds to linear X (linear Y) polarized emission. (e) Streak camera image of TRPL total intensity showing different emission times for X^0, trion, and localized states. Blue (red) corresponds to zero (10 000) counts.

PL emission at later times can be fitted by a simple exponential decay with a characteristic time of 33 ± 5 ps. We have checked carefully using the full dynamic range of our detector that this long-lived decay is not simply due to spectral overlap with other transitions. The origin of this longer time might be linked to a long-lived emission from neutral excitons localized at fluctuations of the crystal potential [42,43]. Note that this type of weak localization is qualitatively different from forming bound states such as the D^0X in GaAs, which might have parallels to the complexes $L1$ and $L2$. Weak laser reflections in our setup lead to weak reexcitation of the sample, giving rise to newly generated X^0 emission that is several orders of magnitude weaker than the initial emission. As the main X^0 signal decays within 4 ps and our detection has a high signal-to-noise ratio, this weak emission is visible when using a logarithmic scale, as in Figs. 3 and 4 (marked by arrows). This reexcitation is unimportant for the trion emission as the

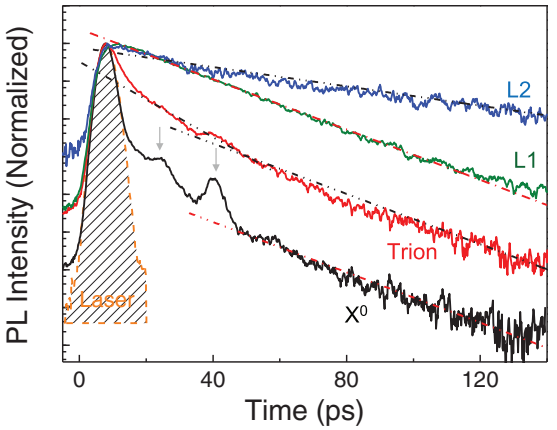

FIG. 3. (Color online) Time-resolved photoluminescence. $T = 4$ K. Normalized PL dynamics (total peak intensity) in log scale for X^0, trion, $L1$, and $L2$. The lines show fits with exponential decays with typical times of 33 ± 5 ps for the second decay time of X^0 (initial time too short to be fitted) and 32 ± 2 ps for $L1$ and 80 ± 6 ps for $L2$. Trion fitted with biexponential decay, with 18 ± 2 and 30 ± 3 ps characteristic decay times. The small peaks superimposed on the X^0 and trion dynamics come from laser reflections marked by arrows.

main, initial emission still largely dominates when the weak laser reflections reach the sample.

The trion PL emission can be fitted by a biexponential decay. We observe no measurable rise time of the trion PL signal within our resolution. The initial trion decay is clearly longer than for the X^0, as can be seen already in Fig. 2(e), and we extract a decay time of about 18 ± 2 ps (see Fig. 3). Similar decay times in differential reflectivity for ML WSe_2 have been found at room temperature in Ref. [44], where trion and X^0 spectrally overlap and cannot be resolved. At longer times we extract an emission with a decay of 30 ± 3 ps, similar to the case of the X^0. In general, the longer emission times allow for a more detailed polarization analysis in the case of the trion compared to the ultrashort X^0 emission. The trion emission time being longer than the X^0 emission time is a trend also observed in III-V [45] and II-VI [46] semiconductor quantum wells, where the longer trion emission time was ascribed to a lowering of the oscillator strength due to a stronger localization. In the ML WSe_2 sample investigated here, the strong optical signature of trion PL at high temperature ($T > 150$ K) hints at the existence of trions independent of spatial localization [see Fig. 1(c), and, for comparison, recent reflectivity measurements on ML WS_2 [47]].

For the peak labeled $L1$ we record a clear, monoexponential decay. The majority of photons resulting from $L1$ recombination are emitted after the main X^0 and trion recombination [see Figs. 2(e) and 3]. The decay time extracted here is 32 ± 2 ps. The considerably less intense transition $L2$ also decays monoexponentially, albeit with a considerably longer characteristic time of 80 ± 6 ps. In temperature dependent measurements, we find for $T > 125$ K that the emission from the $L1$ and $L2$ peaks is negligible compared to the X^0 and the trion lines [compare with Fig. 1(c)]. The emission times measured here for X^0, trion, $L1$, and $L2$ transitions remain essentially constant for the the laser excitation energies used (1.851, 1.893, and 1.968 eV). The exact energy positions and

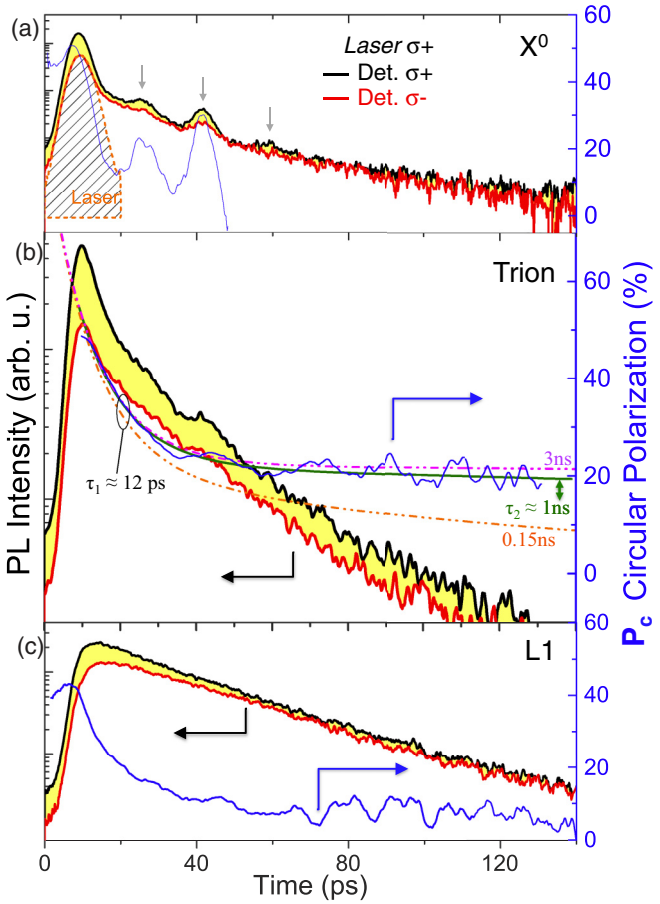

FIG. 4. (Color online) Time-resolved photoluminescence. $T = 4$ K. Laser polarization σ^+. (a) Left axis: X^0 PL emission (in log scale) copolarized (black) and cross-polarized (red) with respect to the excitation laser as a function of time. Right axis: Circular polarization degree of the PL emission. As the PL intensity decays very quickly, we clearly observe a periodic signal of laser reflections, marked by arrows. (b) Same as (a), but for trion emission. The polarization is well reproduced by a biexponential decay using an initial, fast decay time of $\tau_1 = 12$ ps and a long decay time $\tau_2 = 1$ ns (solid green line). Lower bounds (dotted orange line for $\tau_2 = 150$ ps) and upper bounds (dotted purple line for $\tau_2 = 3$ ns) of the slow decay are shown. (c) Same as (a), but for localized exciton emission $L1$.

intensity ratios of $L1$ and $L2$ can vary from sample to sample as they are most likely related to crystal imperfections. Only the behavior of the intrinsic X^0 and trion transitions, which are the focus of the discussion below, is reproducible from sample to sample.

IV. EXCITON VALLEY DYNAMICS

We now discuss the time evolution of the PL polarization that gives access to the valley dynamics. Due to the fast decay time of the main X^0 emission (limited by our temporal resolution), we cannot extract a meaningful polarization decay time. According to recent estimations [33–35], neutral excitons from nonequivalent K valleys in TMDCs are coupled by the Coulomb exchange interaction. This could lead to a rapid decay of the optically initialized circular polarization, in close analogy to neutral exciton depolarization in GaAs quantum wells [32], and will contribute to the fast intervalley relaxation decay observed in 1 ML MoS_2 in pump-probe experiments [30,31]. The coupling of a neutral exciton created with σ^+ light in the K_+ valley to an exciton in the K_- valley is efficient as it does *not* rely on single carrier (electron or hole) spin flips, which are energetically forbidden. In a simple picture, the stationary (time-integrated) polarization is determined by the initially created polarization P_0, the lifetime of the electron-hole pair τ, and the polarization decay time τ_s through $P_c = P_0/(1 + \tau/\tau_s)$ [22,28]. As a direct consequence of the very short emission time τ measured here, even for valley polarization decay times in the ps range, steady-state measurements can still yield a substantial P_c, as in Fig. 2(c). Due to the short X^0 PL emission time (shorter than the temporal resolution of our setup), no meaningful dynamics can be measured for the linear polarization, which corresponds to the valley coherence. The strong valley coherence observed in cw PL in Fig. 2(d) stems mainly from photons emitted within 4 ps.

The initial trion emission time is much longer than the one of the X^0 in Figs. 3 and 4(b); it decays within a few tens of ps, well above the temporal resolution of our experiment. The longer trion emission time allows us to access the time evolution of the valley polarization. The trion polarization decays with 12 ps from 50% down to 20%, followed by a second decay with a characteristic time of the order of 1 ns. The first decay can be linked to the coexistence of trions and excitons during the first few picoseconds and could be due to exchange interaction effects. Once the vast majority of neutral excitons has recombined, the trion polarization evolves differently. This second polarization decay is slower as, in a first approximation, single particle spin flips are needed in addition to valley scattering to change the PL polarization. Given the large spin splittings, these events are scarce and the polarization decays very slowly, as will be discussed below.

Concerning the origin of the initial 12 ps decay, the trion could be either generated directly following photon absorption (phonon assisted process), or by a localized electron capturing a free exciton. This second scenario is unlikely, as within the initial decay of 12 ps the neutral exciton polarization would have already decayed to zero before capture, which is in contradiction with the strong remaining trion valley polarization. Due to the strong Coulomb exchange in this system [34], a trion fine structure is estimated to be in the few meV range, for instance, between trion configurations with the excess electron in the same or different valley with respect to the generated electron-hole pair. Although the linewidth of the PL emission of the trion is considerably smaller in ML WSe_2 than in MoS_2, we cannot extract any trion fine structure splitting for the investigated samples. Clear theoretical predictions for the trion polarization dynamics including Coulomb exchange are currently not available, but it can be expected that the trion fine structure influences the trion polarization dynamics observed here. Also the recently reported electronic exciton-trion coupling could play a role [41].

For times $t \geqslant 40$ ps we can infer a typical decay time of the order of 1 ns; compare in Fig. 4(b) the data and the calculated exponential decay (solid green line). Please note that a typical decay time of 150 ps gives an estimation that is clearly below the observed experimental polarization [orange dashed-dotted line in Fig. 4(b)]. The trion PL polarization dynamics shows clear, experimental proof of the robustness of the optically initialized valley polarization. Measurements carried out at different laser excitation energies show similarly encouraging results. This is in contrast to ML MoS_2, which shows a strong decrease of the PL polarization when the laser excitation energy increases [24,28]. This difference could be due to the fact that the Γ valence states are very close in energy to the K states (a few meV [48]) in MoS_2 whereas for WSe_2 the splitting energy is considerably larger. The emission we labeled $L1$ shows a fast initial polarization decay with a characteristic time of about 13 ps before reaching a polarization plateau as in the trion case, albeit at a smaller value around 8%.

V. CONCLUSION

In conclusion, time-resolved PL experiments in monolayer WSe_2 allow direct access to the valley dynamics by monitoring the charged exciton (trion) emission. We measure a valley polarization decay time of the order of 1 ns. To verify valley stability beyond this time range, pump-probe measurements are needed. Similar results can be expected for ML MoS_2, but are currently far more difficult to extract due to the broader (roughly 3.5×) linewidth at 4 K and also 300 K in exfoliated samples.

ACKNOWLEDGMENTS

We acknowledge partial funding from European Research Council Grant No. 306719 and Programme Investissements d'Avenir ANR-11-IDEX-0002-02, reference ANR-10-LABX-0037-NEXT. We thank I. Gerber and M. M. Glazov for stimulating discussions.

[1] A. K. Geim and I. V. Grigorieva, Nature (london) **499**, 419 (2013).
[2] Z. Y. Zhu, Y. C. Cheng, and U. Schwingenschlögl, Phys. Rev. B **84**, 153402 (2011).
[3] K. F. Mak, C. Lee, J. Hone, J. Shan, and T. F. Heinz, Phys. Rev. Lett. **105**, 136805 (2010).
[4] A. Splendiani, L. Sun, Y. Zhang, T. Li, J. Kim, C.-Y. Chim, G. Galli, and F. Wang, Nano Lett. **10**, 1271 (2010).
[5] W. Zhao, Z. Ghorannevis, L. Chu, M. Toh, C. Kloc, P.-H. Tan, and G. Eda, ACS Nano **7**, 791 (2013).
[6] H. Fang, S. Chuang, T. C. Chang, K. Takei, T. Takahashi, and A. Javey, Nano Lett. **12**, 3788 (2012).
[7] W. Liu, J. Kang, D. Sarkar, Y. Khatami, D. Jena, and K. Banerjee, Nano Lett. **13**, 1983 (2013).
[8] H. Zeng, G.-B. Liu, J. Dai, Y. Yan, B. Zhu, R. He, L. Xie, S. Xu, X. Chen, W. Yao *et al.*, Sci. Rep. **3**, 1608 (2013).
[9] J. S. Ross, P. Klement, A. M. Jones, N. J. Ghimire, J. Yan, D. G. Mandrus, T. Taniguchi, K. Watanabe, K. Kitamura, W. Yao *et al.*, Nat. Nanotechnol. **9**, 268 (2014).
[10] R. S. Sundaram, M. Engel, A. Lombardo, R. Krupke, A. C. Ferrari, Ph. Avouris, and M. Steiner, Nano Lett. **13**, 1416 (2013).
[11] B. Radisavljevic, A. Radenovic, J. Brivio, V. Giacometti, and A. Kis, Nat. Nanotechnol. **6**, 147 (2011).
[12] N. Kumar, S. Najmaei, Q. Cui, F. Ceballos, P. M. Ajayan, J. Lou, and H. Zhao, Phys. Rev. B **87**, 161403 (2013).
[13] D. Xiao, G.-B. Liu, W. Feng, X. Xu, and W. Yao, Phys. Rev. Lett. **108**, 196802 (2012).
[14] A. Rycerz, J. Tworzydlo, and C. J. Beenakker, Nat. Phys. **3**, 172 (2007).
[15] Z. Zhu, A. Collaudin, B. Fauque, W. Kang, and K. Behnia, Nat. Phys. **8**, 89 (2012).
[16] T. Cao, G. Wang, W. Han, H. Ye, C. Zhu, J. Shi, Q. Niu, P. Tan, E. Wang, B. Liu *et al.*, Nat. Commun. **3**, 887 (2012).
[17] X. Li, F. Zhang, and Q. Niu, Phys. Rev. Lett. **110**, 066803 (2013).
[18] G.-B. Liu, W.-Y. Shan, Y. Yao, W. Yao, and D. Xiao, Phys. Rev. B **88**, 085433 (2013).
[19] K. Kosmider, J. W. González, and J. Fernández-Rossier, Phys. Rev. B **88**, 245436 (2013).
[20] A. Kormányos, V. Zólyomi, N. D. Drummond, and G. Burkard, Phys. Rev. X **4**, 011034 (2014).
[21] A. M. Jones, H. Yu, N. J. Ghimire, S. Wu, G. Aivazian, J. S. Ross, B. Zhao, J. Yan, D. G. Mandrus, D. Xiao *et al.*, Nat. Nanotechnol. **8**, 634 (2013).
[22] K. F. Mak, K. He, J. Shan, and T. F. Heinz, Nat. Nanotechnol. **7**, 494 (2012).
[23] G. Sallen, L. Bouet, X. Marie, G. Wang, C. R. Zhu, W. P. Han, Y. Lu, P. H. Tan, T. Amand, B. L. Liu *et al.*, Phys. Rev. B **86**, 081301 (2012).
[24] G. Kioseoglou, A. T. Hanbicki, M. Currie, A. L. Friedman, D. Gunlycke, and B. T. Jonker, Appl. Phys. Lett. **101**, 221907 (2012).
[25] S. Wu, C. Huang, G. Aivazian, J. S. Ross, D. H. Cobden, and X. Xu, ACS Nano **7**, 2768 (2013).
[26] D. Y. Qiu, F. H. da Jornada, and S. G. Louie, Phys. Rev. Lett. **111**, 216805 (2013).
[27] A. Ramasubramaniam, Phys. Rev. B **86**, 115409 (2012).
[28] D. Lagarde, L. Bouet, X. Marie, C. R. Zhu, B. L. Liu, T. Amand, P. H. Tan, and B. Urbaszek, Phys. Rev. Lett. **112**, 047401 (2014).
[29] T. Korn, S. Heydrich, M. Hirmer, J. Schmutzler, and C. Schüller, Appl. Phys. Lett. **99**, 102109 (2011).
[30] C. Mai, A. Barrette, Y. Yu, Y. G. Semenov, K. W. Kim, L. Cao, and K. Gundogdu, Nano Lett. **14**, 202 (2014).
[31] Q. Wang, S. Ge, X. Li, J. Qiu, Y. Ji, J. Feng, and D. Sun, ACS Nano **7**, 11087 (2013).
[32] M. Z. Maialle, E. A. de Andrada e Silva, and L. J. Sham, Phys. Rev. B **47**, 15776 (1993).
[33] T. Yu and M. W. Wu, Phys. Rev. B **89**, 205303 (2014).
[34] H. Yu, G. Liu, P. Gong, X. Xu, and W. Yao, Nat. Commun. **5**, 3876 (2014).
[35] M. M. Glazov, T. Amand, X. Marie, D. Lagarde, L. Bouet, and B. Urbaszek, Phys. Rev. B **89**, 201302 (2014).
[36] Very similar times have been found at $T = 300$ K in differential reflection where trion and X^0 emissions are merged [44].

[37] K. S. Novoselov, D. Jiang, F. Schedin, T. J. Booth, V. V. Khotkevich, S. V. Morozov, and A. K. Geim, Proc. Natl. Acad. Sci. USA **102**, 10451 (2005).

[38] G. Sallen, B. Urbaszek, M. M. Glazov, E. L. Ivchenko, T. Kuroda, T. Mano, S. Kunz, M. Abbarchi, K. Sakoda, D. Lagarde *et al.*, Phys. Rev. Lett. **107**, 166604 (2011).

[39] Note that this assumption is not critical for ML WSe_2. The trion valley polarization is protected by the large spin splitting Δ_{SO} in the valence band ($\Delta_{SO}^{VB} \approx 430$ meV [2] at $k = K_{\pm}$) and the conduction band ($\Delta_{SO}^{CB} \approx 30$ meV [18,19]), where Δ_{SO}^{CB} still needs to be confirmed experimentally [49]. Charge tunable structures [21] are ideal to investigate alternatively the positively charged trion.

[40] G. Wang, X. Marie, I. Gerber, T. Amand, D. Lagarde, L. Bouet, M. Vidal, A. Balocchi, and B. Urbaszek, arXiv:1404.0056.

[41] A. Singh, G. Moody, S. Wu, Y. Wu, N. J. Ghimire, J. Yan, D. G. Mandrus, X. Xu, and X. Li, Phys. Rev. Lett. **112**, 216804 (2014).

[42] B. Deveaud, F. Clérot, N. Roy, K. Satzke, B. Sermage, and D. S. Katzer, Phys. Rev. Lett. **67**, 2355 (1991).

[43] T. Amand, J. Barrau, X. Marie, N. Lauret, B. Dareys, M. Brousseau, and F. Laruelle, Phys. Rev. B **47**, 7155 (1993).

[44] Q. Cui, F. Ceballos, N. Kumar, and H. Zhao, ACS Nano **8**, 2970 (2014).

[45] G. Finkelstein, V. Umansky, I. Bar-Joseph, V. Ciulin, S. Haacke, J.-D. Ganière, and B. Deveaud, Phys. Rev. B **58**, 12637 (1998).

[46] E. Vanelle, M. Paillard, X. Marie, T. Amand, P. Gilliot, D. Brinkmann, R. Lévy, J. Cibert, and S. Tatarenko, Phys. Rev. B **62**, 2696 (2000).

[47] A. Chernikov, T. C. Berkelbach, H. M. Hill, A. Rigosi, Y. Li, O. B. Aslan, D. R. Reichman, M. S. Hybertsen, and T. F. Heinz, arXiv:1403.4270.

[48] A. Kormányos, V. Zólyomi, N. D. Drummond, P. Rakyta, G. Burkard, and V. I. Fal'ko, Phys. Rev. B **88**, 045416 (2013).

[49] Y. Zhang, T.-R. Chang, B. Zhou, Y.-T. Cui, H. Yan, Z. Liu, F. Schmitt, J. Lee, R. Moore, Y. Chen *et al.*, Nat. Nanotechnol. **9**, 111 (2014).